Acc. Chem. Res. **2004,** *37,* 989−998

A Thermodynamic "Vocabulary" for Metal Ion Interactions in Biological Systems

M. T. RODGERS
Chemistry Department, Wayne State University, Detroit, Michigan 48202

P. B. ARMENTROUT*
Chemistry Department, University of Utah, Salt Lake City, Utah 84112

Received July 13, 2004

ABSTRACT

This Account focuses on metal ion−ligand complexes of biological relevance and measurements of the bond dissociation energies (BDEs) of such species. These complexes yield thermochemistry that begins to provide a thermodynamic "vocabulary" for thinking quantitatively about the strength of interactions in biological systems. The method utilized is threshold collision-induced dissociation in a guided ion beam tandem mass spectrometer. Accurate determination of BDEs requires attention to many details of the experiments and data analysis, as outlined here. Trends in metal ion−ligand BDEs are examined as a function of the metal ion, ligand, and extent of ligation. We elucidate the importance of ion−dipole and ion-induced dipole interactions, chelation, conformation, tautomeric form, steric interactions, and electronic effects such as hybridization and promotion. Interactions of metal ions with nucleobases and amino acids are quantified and the effects of hydration on these values are explored for the amino acid systems. Although data limitations restrict the present discussion to monocations, the trends elucidated here should be relevant to multiply charged metal ions, for which data is forthcoming.

I. Introduction and Motivations

The primary structure of biological molecules is determined by the covalent bonds that link amino acids into proteins, sugars into carbohydrates, and nucleobases, sugars, and phosphate esters into nucleic acids. Secondary, tertiary, and quaternary structures and the biochemical function of these biopolymers are controlled by noncovalent interactions among the constituent groups and with various metal ions, substrates, and solvents. Further, noncovalent interactions are responsible for condensation and solvation. Because noncovalent interactions are generally much weaker than covalent bonds, they provide biochemical systems the flexibility to vary structure and function with changes in the local environment. Despite the prominent roles that noncovalent interactions play in biochemistry, experimental determinations of the strengths of such interactions are presently limited, largely because of the numerous interactions involved in any biological system. One means to address this lack of thermodynamic data is to quantitatively evaluate pairwise interactions between individual components of biological systems, both for simple systems and for more complex interactions that evolve with larger systems. These pairwise interactions along with the more subtle thermodynamic aspects of complex systems can then be combined to provide accurate estimates of the overall systems. Progress toward the development of such a thermodynamic "vocabulary" is outlined here.

In this Account, we focus on experimental studies of metal ion−ligand binding, one type of noncovalent bonding interaction of biological interest. Obtaining accurate thermochemistry on metal−ligand systems remains a state-of-the-art enterprise for both experiment and theory; hence, theoretical results will be introduced only to enhance discussion of the experimental studies. Much of the available thermodynamic data has been generated using threshold collision-induced dissociation (TCID), which is described. Trends in the bond dissociation energies (BDEs) for a variety of metal−ligand systems are discussed. Simple systems that bind via noncovalent σ and π interactions are first described and then used to evaluate metal ions interacting with nucleobases and amino acids. The effects of hydration are also examined and can be viewed as the bridge between gas-phase and solution-phase thermodynamic information.

At this time, such data are available primarily for metal monocations, whereas many metals in biological systems, for example, the alkaline earths and transition metals, participate as multiply charged ions. Such species will bind much more tightly to ligands because of the enhanced electrostatic potential and smaller ionic radius, but once the electronic configuration is considered, multiply charged ions should follow the same trends (periodic, variations with ligand identity, solvation effects) elucidated below for the singly charged analogues.

It will be taken for granted in this Account that the values obtained from TCID measurements are accurate. This has been verified[1] for a wide range of simple systems where reliable thermochemistry is available from other methods and for the more complex systems by comparison with results of ab initio theory. Indeed, one of the key contributions of such studies is to establish thermodynamic benchmarks that should prompt refinements in theoretical approaches for complex biological systems.

II. Experimental Methods

For results reviewed here, thermodynamic information is obtained from TCID experiments in a guided ion beam tandem mass spectrometer (GIBMS). In such experiments,

Mary T. Rodgers was born in Chicago, IL, on July 7, 1963. She received a B.S. degree from Illinois State University and a Ph.D. from Caltech, where she worked with A. Kuppermann. After postdoctoral positions at Caltech with J. L. Beauchamp and the University of Utah with P. B. Armentrout, she joined the faculty at Wayne State University, where she is presently an Associate Professor of Chemistry.

Peter B. Armentrout was born in Dayton, OH, on March 13, 1953. He received his B.S. degree from Case Western Reserve University and a Ph.D. from Caltech, where he worked with J. L. Beauchamp. After a postdoctoral position at Bell Laboratories in Murray Hill, NJ, he joined the faculty at the University of California at Berkeley. In 1987, he moved to the University of Utah, where he is currently a Distinguished Professor of Chemistry, Cannon Fellow, and Department Chair.

* Corresponding author. Mailing address: 315 S. 1400 E. Rm. 2020, Salt Lake City, UT 84112.

10.1021/ar0302843 CCC: $27.50
Published on Web 11/05/2004

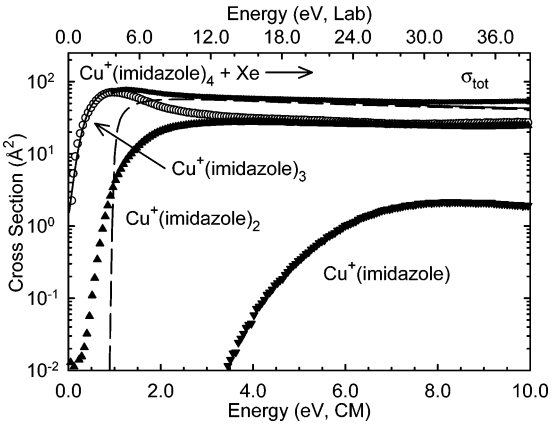

FIGURE 1. Cross sections for collision-induced dissociation of Cu^+-(imidazole)$_4$ with Xe as a function of kinetic energy in the center-of-mass (lower *x*-axis) and laboratory (upper *x*-axis) frames. The lines show the best fit to the data as described in the text.

the kinetic energy dependence of the CID reaction 1 is measured as shown in Figure 1 for the Cu^+(imidazole)$_4$

$$M^+(L)_x + Xe \rightarrow M^+(L)_{x-1} + L + Xe \qquad (1)$$

complex.[2] The reaction cross section increases with energy, clearly indicating that reaction 1 is endothermic. Loss of two and three imidazole ligands follows at higher energies. For such heterolytic bond cleavages of ionic systems in the gas-phase, there should be no reverse activation barrier.[3] Thus, the reaction threshold directly provides the BDE, $D_0[(L_{x-1})M^+-L]$. Details of the GIBMS instrumentation and data analysis have been discussed previously.[4−7] Important features for obtaining accurate thermodynamic information are highlighted here.

Instrumentation. Accurate determination of BDEs requires specialized instrumentation such as the GIBMS found in our laboratories.[4,8] Briefly, these experiments involve carefully creating ions with a known internal energy distribution, in our case, Maxwell−Boltzmann at 298 K. Desired ions are selected by a magnetic mass spectrometer and focused into an interaction region where the kinetic energy is varied over a wide range. Experiments at several pressures of the neutral reagent allow extrapolation to zero pressure, corresponding to rigorous single collision conditions.[7] The collision gas should provide efficient kinetic to internal energy transfer, making Xe preferred.[5,7] The interaction region is surrounded by a radio frequency (rf) octopole ion beam "guide",[9] which ensures well-defined collision energies and efficient ion collection. After leaving the octopole, reactant and product ions are mass-separated, and their absolute intensities are measured. The raw data are converted to absolute reaction cross sections versus kinetic energy in the center-of-mass (CM) frame,[4] for example, Figure 1. Cross sections can be viewed as a microscopic measure of the reaction probability. The absolute zeros of the cross section and energy scales are measured.

Data Analysis. Reaction thresholds are determined by analyzing the experimental cross sections with a model that includes contributions of reactant states (vibrational, rotational, or electronic, or combinations of these) and the kinetic energy distributions of both reactants.[10] Statistical kinetic theories[11] are used to account for kinetic shifts resulting from collisionally activated molecules having lifetimes comparable to the available experimental time scale.[6,12,13] For metal ions ligated by different molecules, direct competition between parallel reaction pathways should be explicitly considered.[14]

After including all of these effects, the parameters of the model (including the threshold energy) are optimized to give the best reproduction of the data, as illustrated in Figure 1. The apparent threshold of the data (essentially 0 eV) differs appreciably from the 0 K threshold (0.75 eV) obtained from modeling (dashed line) because of the energy content of the reactants along with kinetic shifts. Convolution of this model over the energy distributions (solid line) reproduces the data extremely well over a wide range of magnitudes and energies. This procedure typically yields absolute metal−ligand BDEs that have proved accurate for a wide variety of systems covering a wide dynamic range, 15−400 kJ/mol, with uncertainties of 2−10 kJ/mol.[1]

Theoretical Support. Ab initio theoretical calculations are generally used to determine the vibrational frequencies and rotational constants of the dissociating complexes and products, to visualize structures of these species, and to calculate energies for comparison to experimental BDEs. The latter can help identify electronic or structural isomers but requires electron correlation (MP2 or density functional methods) and a reasonably sized basis set, for example, 6-31G* for geometry optimizations and 6-311+G-(2d,2p) for single-point energies. Accurate theoretical BDEs require corrections for zero-point energies and basis set superposition errors, although the full counterpoise correction may be excessive.[15−17]

Comparison with Other Methods. Metal−ligand BDEs have also been measured by several other experimental techniques. Absolute thermochemistry can be measured by temperature-dependent equilibrium methods,[18−20] blackbody-infrared radiative dissociation (BIRD),[21−23] and radiative association (RA).[24] Relative measurements can be accomplished using equilibrium[25] and kinetic method (KM) procedures.[26,27] The dynamic ranges of equilibrium, BIRD, and RA methods are narrower than TCID (40−200 kJ/mol or less). The primary limitation of TCID (as well as BIRD, RA, and KM) is its model dependence (which is no more severe than that of the Arrhenius equation), whereas equilibrium studies are well-established thermodynamic methods.

III. σ Bonding Systems

Metal Dependence. Among the most important, ubiquitous, and simplest ligands is water. Metal cations bind to water at oxygen with a metal−oxygen bond lying along the dipole moment of water. For alkali cations, the BDE to Li^+ is highest and declines gradually to Cs^+, as shown in Figure 2 for the first three alkalis. The stable rare-gas-like electronic structure of the alkali metal ions means that

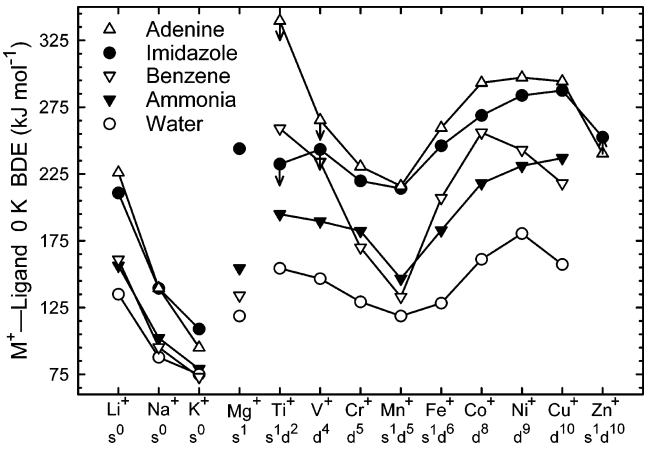

FIGURE 2. Periodic trends in the binding of metal ions to several ligands. Arrows indicate upper or lower limits. Lines join elements adjacent in the periodic table. Data are listed in Table S1, Supporting Information.

they act as spherical centers of charge with radii of 0.70, 0.98, 1.33, 1.49, and 1.69 Å for Li^+, Na^+, K^+, Rb^+, and Cs^+, respectively.[28] These radii control the M−O bond length, which modifies the electrostatic interaction such that longer bond lengths lead to weaker interactions.

If such simple electrostatic ideas always worked, then BDEs should always be inversely related to metal ion radii, whereas the electronic structure of the metal ion demonstrably influences metal−ligand BDEs. For example, Mg^+ has a single valence s electron, which might be anticipated to decrease the BDE because of Pauli repulsion with the electron-donating ligand. In contrast, BDEs to water are observed to increase from Na^+ to Mg^+, Figure 2.[29] This trend can be explained by sp-hybridization,[30] which costs energy but allows the electron density to polarize away from the water ligand, exposing a higher nuclear charge and increasing the electrostatic interaction.

The effect of orbital occupancy can also be observed in BDEs of water to transition-metal monocations, Figure 2. Here, the electrostatic contributions to the BDEs increase from left to right across the periodic table because the metal ion radii decrease.[31,32] However, there are much larger variations in the BDEs than this monotonic prediction, which can be understood by realizing that water is a strong σ-donor and a weak π-donor.[31−34] For a $M^+(H_2O)$ complex lying in the xz plane, the ligand field induces metal orbitals having energies in the order $d\delta(xy) \approx d\delta'(x^2 - y^2) < d\pi(xz) < d\pi'(yz) < d\sigma(z^2) <$ s. When $M^+ = Ti^+$ and V^+, the lowest four orbitals are progressively singly occupied and the BDE decreases slightly as the weakly antibonding $d\pi'$ orbital is occupied. Occupation of the more antibonding $d\sigma$ orbital by $Cr^+(H_2O)$ decreases the BDE further, and in $Mn^+(H_2O)$, there is strong Pauli repulsion between the occupied s orbital and the ligand. All these complexes have high-spin configurations that maximize the quantum mechanical exchange energy. Note that BDEs of water to $Mn^+(s^1d^5)$ and $Mg^+(s^1)$ are comparable, consistent with both metal ions having singly occupied s orbitals and utilizing sp-hybridization to enhance the bonding. $Fe^+(H_2O)$ has a BDE slightly greater than $Mn^+(H_2O)$ because the additional electron occupies the nonbonding ($d\delta$) orbital, and Fe^+ is smaller. For Co^+, Ni^+, and Cu^+, BDEs increase substantially because they have d^n configurations with no s-electron, thereby avoiding the strong Pauli-repulsion. The decrease from $Ni^+(H_2O)$ to $Cu^+(H_2O)$ can be attributed to the unfavorable double occupation of the $d\sigma$ orbital.

The BDEs of transition-metal cation−water complexes are relatively large compared to those for alkali and alkaline earth metal ions, Figure 2. This observation can be explained using sd-hybridization, which, like sp-hybridization, removes electron density from the metal−ligand bonding axis. This increases the effective nuclear charge seen by the ligand, thereby increasing the BDEs. Less energy is required for sd-hybridization than sp-hybridization because s and d orbitals are comparable in energy, whereas p orbitals lie higher.[30] Because of the symmetry of d orbitals, the electron density is placed in a direction perpendicular to the bonding axis.

Ligand Dependence: Ammonia, Azoles, and Azines. Metal−ligand BDEs also vary considerably with the properties of the ligand, generally scaling with the number of electrons donated, the magnitude and alignment of the ligand dipole (or local dipole at the bonding site), and the polarizability of the ligand. Other effects include chelation, ligand conformation, and sterics. It should be realized that these effects can rarely be isolated completely and the overall trends in BDEs are the culmination of several of these effects. Here the basic trends are illustrated using several nitrogen-based molecules, species that can be viewed as building blocks of biological molecules, for example, nucleobases.

Previously we have shown that the BDEs of metal−ligand systems generally correlate with calculated bond lengths (R).[1] These plots indicate potentials having a R^{-3} dependence, consistent with ion-locked dipole interactions, as appropriate for ligands having permanent dipoles oriented along the metal−ligand bond. For some ligands, however, the preferred binding site (usually the best electron donor) does not lie along the dipole moment of the molecule. For example, in pyrimidine (c-1,3-$C_4H_4N_2$) and 2H-1,2,3-triazole (c-$C_2H_3N_3$), the metal ion binds to a lone pair of electrons on one of the equivalent nitrogen atoms, but the overall dipole moment is oriented toward a CH group. In such cases, BDEs are smaller than might be anticipated from the magnitude of the dipole moment.[1]

Comparison of BDEs of metal cations with water and ammonia[35] is also illustrative, Figure 2. BDEs to ammonia are higher than those to water, even though the dipole moment of water is larger and R(MO) < R(MN) because the position of the ammonia dipole is closer to the metal ion than that of water.[31] Further, BDEs for late first-row transition metals (Co^+−Cu^+) with ammonia are roughly 32% greater than those for early metals (Ti^+−Cr^+), whereas for $M^+(H_2O)$ complexes, the enhancement is only 16%. This periodic effect results from differences in the π-donor abilities of H_2O and NH_3, the latter having no π-interactions. For early metals, H_2O π-donates, thereby enhancing

their BDEs. The effectiveness of this π-donation is progressively reduced as the dπ orbitals on late metals are occupied.

The strongest long-range interaction between metal ions and ligands is the ion−dipole interaction, but a significant contribution comes from ion-induced dipole interactions. These generally dominate when the ligand has no permanent dipole. The induced dipole varies with the polarizability of the ligand, as illustrated by increases in the BDEs of metal ions to alcohols as the chain length increases.[1] Another example is nitrogen heterocycles where the polarizability decreases as the number of nitrogen atoms increases. BDEs to alkali metal ions follow the order pyridine (*c*-C_5H_5N) > pyrimidine (*c*-1,3-$C_4H_4N_2$) ≈ pyrazine (*c*-1,4-$C_4H_4N_2$) > *s*-triazine (*c*-1,3,5-$C_3H_3N_3$).[36] However, the BDEs of alkali ions to pyridazine (*c*-1,2-$C_4H_4N_2$) are higher than to the 1,3 and 1,4 isomers, even though their polarizabilities are comparable.[36] In all these systems, the metal ion binds to a nitrogen lone pair in the plane of the ligand, but in pyridazine, it bridges the two closely spaced nitrogen atoms. Li^+ and Na^+ bind pyridazine more strongly than pyrimidine and pyrazine by ∼53% ± 4%, whereas K^+ shows an enhancement of 90% ± 4% because the larger potassium ion overlaps both nitrogen lone pairs more effectively. Other clear-cut examples of chelation are observed for the nucleobases and amino acids, as described below.

Of course, one of the complexities of biological molecules as ligands is the existence of multiple conformers and tautomers. For example, 1,2,3-triazole, 1,2,4-triazole, and tetrazole, the five-membered N-heterocycles, are known to exist in two tautomeric forms distinguished by the position of the N−H bond. Here, metal ions should bind most tightly to the tautomer having the higher dipole moment, but the other tautomer is more stable in the gas phase. Comparisons of experimental and theoretical BDEs demonstrate that the complexes formed in the gas phase between alkali cations and these three azoles all correspond to complexes with the more stable gas-phase tautomer.[37] No tautomerization was evident during complex formation or dissociation, consistent with a large barrier to tautomerization in the gas phase.

IV. π Bonding Systems

Figure 2 also shows BDEs for first row transition-metal ions to benzene.[38] The periodic trends in these BDEs are roughly parallel those for the other ligands shown, although the variations are stronger. Benzene has a relatively high BDE because it is a six-electron donor with a large polarizability. The binding is largely electrostatic with contributions from metal π back-donation,[39] such that the d orbitals split into $de_2(\delta)$ < $da_1(\sigma)$ < $de_1(\pi^*)$ molecular orbitals. Progressing from Ti to Cr (with 3−5 d-electrons) and from Co to Cu (with 8−10 d-electrons), the π^* antibonding orbitals are increasingly occupied. The π^* occupation leads to decreasing BDEs, which is even more obvious for the $(C_6H_6)M^+-C_6H_6$ BDEs.[38] Fe^+ binds more strongly than Cr^+ because there are two additional electrons in the bonding de_2 molecular orbital, indicating that $Fe^+(C_6H_6)$ has a low-spin quartet state (correlating to the d^7 configuration). The weak bond for Mn is again a consequence of the occupied 4s orbital.

Benzene, azines, and azoles are aromatic rings capable of acting as six-electron π-donors. A priori, it is not clear whether a two-electron σ-bond or a more diffuse six-electron π-interaction would be more favorable. Comparison of the metal-ion BDEs of benzene, azines, and azoles demonstrates that in-plane σ-interactions are preferred over π-complexation whenever a lone pair of electrons lies in the plane.[37,40,41] This is true for all azines and azoles examined thus far except pyrrole (*c*-C_4NH_5) and 1-methylpyrrole.

Table 1. 0 K Bond Dissociation Energies Measured by TCID of Selected Metal Ions with Nucleobases and Amino Acids (in kJ/mol)[a]

ligand	Li^+	Na^+	K^+
imidazole	211(10)[b]	140(4)[b]	109(6)[b]
adenine (A)	226(6)[c]	140(4)[c]	95(3)[c]
uracil (U)	212(6)[c]	135(3)[c]	104(3)[c]
1-methyluracil	234(7)[d]	151(4)[d]	111(3)[d]
3-methyluracil	221(7)[d]	144(4)[d]	108(3)[d]
5-methyluracil (thymine, T)	210(7)[c]	135(4)[c]	104(4)[c]
6-methyluracil	222(7)[d]	137(6)[d]	109(5)[d]
1,3-dimethyluracil	240(8)[d]	154(5)[d]	119(3)[d]
5,6-dimethyluracil	234(7)[d]	137(5)[d]	113(3)[d]
5-fluorouracil	199(5)[e]	149(4)[e]	110(4)[e]
5-chlorouracil	243(8)[e]	141(3)[e]	104(3)[e]
6-chlorouracil	230(8)[e]	140(4)[e]	98(2)[e]
5-bromouracil	236(5)[e]	142(5)[e]	110(2)[e]
5-iodouracil		140(4)[e]	98(2)[e]
2-thiouracil		140(3)[f]	103(3)[f]
4-thiouracil		126(5)[f]	97(6)[f]
2,4-dithiouracil		100(6)[f]	81(3)[f]
5-methyl-2-thiouracil		142(6)[f]	101(3)[f]
6-methyl-2-thiouracil		144(4)[f]	107(4)[f]
glycine	220(9)[g]	164(6)[h]	121(4)[i]
proline	279(10)[j]	186(4)[j]	144(4)[j]
methionine	321(17)[k]	202(11)[k]	142(11)[k]
phenylalanine		206(7)[l]	150(6)[l]
tyrosine		209(10)[l]	155(9)[l]
tryptophan		217(8)[l]	165(6)[l]

[a] Uncertainties in parentheses. [b] Reference 37. [c] Reference 43. [d] Reference 44. [e] Reference 45. [f] Reference 46. [g] Reference 15. [h] Reference 16. [i] Reference 49. [j] Reference 17. [k] Reference 50. [l] Reference 51.

V. Nucleobases

To understand noncovalent interactions with nucleic acids, quantitative studies of metal ions binding to nucleobases, sugars, and phosphates would all be desirable. Previous efforts have focused on the nucleobases,[42] and TCID studies include thymine,[43] uracil,[43] substituted uracils,[44−46] and adenine,[43,47] (Table 1), whereas studies of cytosine, guanine, and phosphate esters are currently being pursued.

Uracil and Substituted Uracils. BDEs of Li^+, Na^+, and K^+ bound to uracil, thymine, and several substituted uracils have been measured using TCID.[43−46] Methylation (1-, 3-, 5-, 6-), halogenation (6-), and thio-substitution (2-), or combinations of these do not significantly influence the BDEs or alter the preferred binding sites (O4, Figure 3). Surprisingly, N-methylation (1-, 3-) enhances

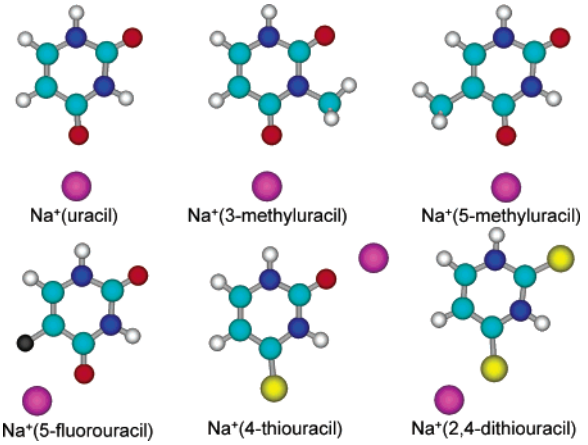

FIGURE 3. MP2(full)/6-31G* optimized geometries of sodium cations bound to various substituted uracils.

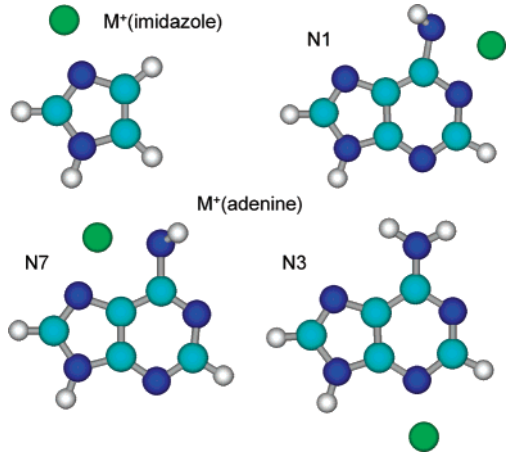

FIGURE 4. B3LYP/6-31G* optimized geometries of copper cations bound to imidazole and adenine.

thebinding more significantly than C-methylation (5-, 6-), in contrast to expectations based solely upon changes in polarizability and dipole moment of the nucleobase. For most systems, 5-halogenation increases the BDE, which likely arises from chelation with the halogen substituent and more optimal alignment with the dipole moment. In contrast, 6-halogenation weakens the interaction because the dipole moment is significantly reduced and chelation is not possible. 4-Thio-substitution greatly reduces the binding interaction because the metal binds to the less favorable oxygen site (O2). For 2,4-dithiouracil, more pronounced decreases in BDEs are observed because binding to the S4 site increases the metal−ligand bond distances and the metal ion binds out of the plane.

Adenine. BDEs of Li^+, Na^+, and K^+ bound to adenine have been measured using TCID.[43] The complexes are planar with the metal ion binding to the nitrogen lone pairs, Figure 4, as can be anticipated from the azine results. A key observation is that these ions bind most strongly to adenine at the N7 site, suggesting that imidazole acts as a good model for binding in this system. Additional stabilization is achieved via chelation to the amino group, Figure 4, which can be modeled by ammonia. Given the strengths of M^+(imidazole) and $M^+(NH_3)$ bonds, Figure 2, the chelation interaction of adenine surprisingly results in only a small increase in the BDE relative to imidazole for Li^+, none for Na^+, and a decrease for K^+. This is because the metal ion is no longer optimally aligned with either binding site, and chelation requires rotation of the amino group and the concomitant loss of π-resonance stabilization (estimated as ~55 kJ/mol). Because this energetic cost is fixed, the relative BDEs of adenine and imidazole to the alkali cations determine whether chelation strengthens or weakens the bond. Binding at the N1 site is comparable in strength as it also involves chelation, whereas the N3 binding site is weaker because no chelation is possible.

Studies of M^+(adenine) complexes have also been conducted for all first-row transition-metal ions: Sc^+−Zn^+.[47] Figure 2 compares the measured BDEs to those previously studied for simple N-donor ligands, NH_3 and imidazole. Because of the influence of sd-hybridization on the transition-metal ions, the relative energies of different binding sites on adenine differ from those of the alkali ions. Theoretical calculations for the Cu^+(adenine) complex agree that binding at the N7 site is favorable, with N1 binding much weaker. The energetics of binding at the N3 site relative to N7 are theory-dependent and range from comparable stability to less stable by 5−17 kJ/mol. Compare this stability ordering, N7 > N3 ≫ N1, with that for the alkali metal cations, N7 ≈ N1 ≫ N3. The change occurs because sd-hybridization does not allow as strong a chelation interaction as that for the spherical alkali ions. Further the preferred 180° directionality of bidentate binding to transition-metal ions (see below) results in stronger binding at N7 (where ∠N−Cu−N = 102°) than at N1 (∠N−Cu−N = 73°).

Implications for DNA Duplex Stability. An interesting consequence of these results is predictions for stability changes in DNA duplexes in the absence of metal ions. Results for substituted uracils indicate that because substitution increases the polarizability, stronger π-stacking interactions can be anticipated. With regard to A:T (A:U) nucleic acid base pairs, the thermochemistry measured here suggests that most substituents will either have no affect or slightly strengthen hydrogen-bonding interactions because the O4 site becomes more basic and the N3 site becomes more acidic. 3-Methylation is an obvious exception because it blocks one of the hydrogen-bonding sites. Thio-substitution also adversely affects hydrogen-bonding because sulfur is less basic than oxygen, the C═S bond is elongated compared to C═O, and the preferred binding site to sulfur is out of the plane.

Our results also allow some speculation regarding metal-induced changes in duplex stability, specifically A::T (A::U) nucleic acid base pairs. Metal ion binding at the N3 site of adenine should not disrupt the planar hydrogen-bonding in an AT (AU) base pair and should enhance the bonding by increasing the acidity of the amino group. In contrast, binding of Li^+, Na^+, transition-metal ions, and certainly multiply charged ions to adenine at the N7/NH_2 chelation site is strong enough to disrupt hydrogen bonding in A::T, because a single hydrogen-bond energy in an AT base pair is ~27 kJ/mol.[48] However, calculations

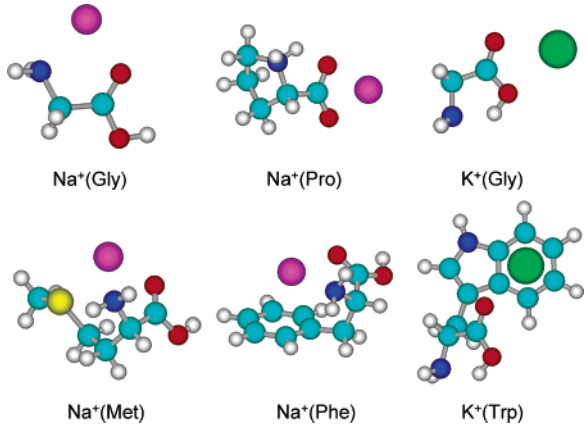

FIGURE 5. MP2(full)/6-31G* and B3LYP/6-31G* optimized geometries of metalated amino acids.

indicate that distortion of the planar base pair permits the chelation and the hydrogen bonds to coexist, leading to a similar enhancement in the base-pair bonding as N3 binding. Stronger enhancements were found for binding metal ions to U at the O2 and O4 sites, but this appears to be a result of strong nonplanar distortions of the base pair, which permit the metal ion to interact with both U and A (at the O2 + N3 or O4 + NH_2 sites). Although two and one hydrogen bonds, respectively, are maintained, their strength is compromised by the nearly perpendicular arrangement of the two bases. Such large geometric distortions will impact π-stacking interactions in nucleic acids, such that the preferred binding site for metal ions may be the N3 site of adenine. Our results also suggest that early transition metals (the periodic groups containing Sc^+, Ti^+, and V^+) may activate covalent bonds leading to DNA damage.[47] Similar destructive behavior might also be expected for any transition-metal ion (such as a multiply charged species) that is not adequately solvated to reduce its reactivity.

VI. Amino Acids

The absolute[15−17,49−51] and relative[27,52,53] BDEs of metal ions (Li^+, Na^+, K^+, and Cu^+) to a variety of amino acids have been measured. Additional studies have extended this work to include small peptides.[54,55] Further work on common coordinating amino acids at protein−metal ion binding sites (histidine, cysteine, aspartic acid, and glutamic acid) is in progress.

Glycine. The BDEs of glycine with Li^+,[15] Na^+,[16] and K^+ [49] (Table 1) have been examined in some detail by comparing this thermochemistry to that of five comparably sized molecules that contain the functional components of glycine both singly (propanol, propylamine, and methyl ethyl ketone) and in pairs (ethanol amine and propionic acid). These comparisons demonstrate that the primary binding site is the carbonyl with a BDE reduced (by 8−25 kJ/mol) by the inductive effect of OH in the carboxylic acid group. For Li^+ and Na^+, chelation to the amino group enhances the bonding (by ~50 kJ/mol) and makes glycine act as a bidentate ligand, Figure 5. An important subtlety of this interaction is that sp^2-hybridization at the carbon center of the carboxylic acid group introduces steric constraints on the ligand conformation, reducing its bond strength to metal ions by >10 kJ/mol. In contrast, the more-weakly bound K^+ is found to preferentially attach to glycine at the two carboxylic acid oxygens, Figure 5. This reduces the conformational strain introduced by metal ion binding and avoids the nitrogen site, a relatively weak binding site for K^+.[49] The zwitterionic structure, the ground-state conformation in solution, is calculated to be higher in energy by 17, 8, and 7 kJ/mol for Li^+, Na^+, and K^+, respectively.

Proline. Proline is the only naturally occurring amino acid with a secondary backbone nitrogen. As such, the zwitterionic structure is particularly stable. Calculations find that proline complexes with Li^+, Na^+, and K^+ are all zwitterionic with the metal attached to the carboxylate acid group, Figure 5 and Table 1.[17] Compared with zwitterionic structures for glycine, proline binds these alkalis more strongly by 76, 26, and 30 kJ/mol, respectively. One intriguing aspect of this particular study was comparison to four- and six-membered ring analogues of proline, which are found to bind the three alkali metal ions as zwitterions but less tightly than proline. Given the greater conformational flexibility of the six-membered ring, this is perhaps surprising but can be rationalized by the ability of proline to form a strong N−H···O hydrogen bond without distorting the ring. In the six-membered ring, such a hydrogen bond can only be formed if the ring distorts, which is avoided by forming weaker bifurcated NH_2···O hydrogen bonds. Although speculative, it seems possible that similar structural and energy considerations may be influential in how proline evolved as the naturally occurring cyclic amino acid.

Methionine. TCID measurements of the BDEs of methionine, where the R-group is $-C_2H_4SCH_3$, to Li^+, Na^+, and K^+ have been performed, Table 1.[50] The BDEs are substantially larger than those to glycine or proline because methionine acts as a tridentate ligand binding to the amide, carbonyl, and sulfur, Figure 5. This third interaction enhances the binding considerably compared to glycine with a strong metal ion dependence (46% for Li^+, 23% for Na^+, and 13% for K^+).

Phenylalanine, Tyrosine, and Tryptophan. Like methionine, the three aromatic amino acids have a side chain that can act as a third binding site. For phenylalanine and tryptophan, the aromatic side chains are π-binding sites, whereas the metal ion can bind to tyrosine either at the benzene ring or at the phenolic oxygen.[51] Thus, M^+−ligand interactions in these complexes involve both σ- and π-donation, Figure 5. Calculations indicate that Li^+, Na^+, and K^+ form tridentate complexes binding to the amide, carbonyl, and aromatic rings of phenylalanine and tyrosine. Tridentate structures are also found for Li^+ and Na^+ binding to tryptophan, whereas K^+ binds via a bidentate interaction with the carbonyl and the aromatic ring. Because of the constrained geometries, a simple sum of the pairwise interactions overestimates the final BDEs (by about 25−35%), but such thermodynamic information is precisely what is needed to quantify how pairwise

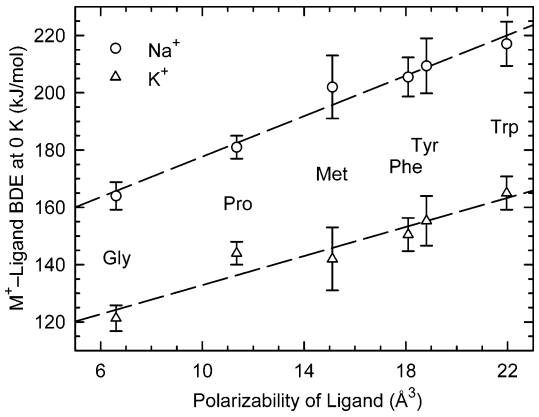

FIGURE 6. Measured M^+—AA BDEs at 0 K (in kJ/mol) versus estimated polarizability. Lines are linear regression fits to the data for each alkali metal cation.

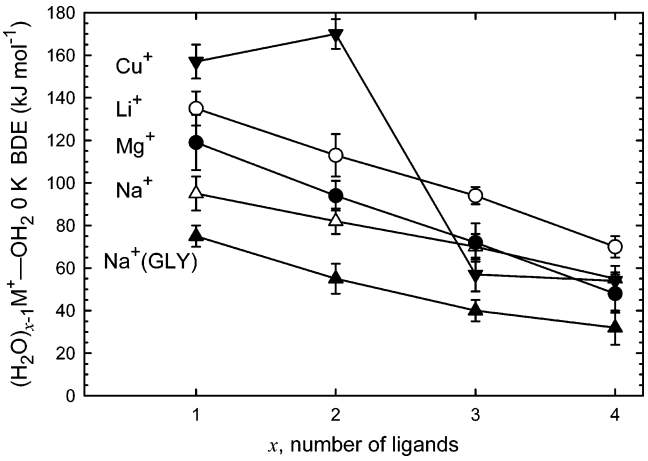

FIGURE 7. Trends in the sequential BDEs of $M^+(H_2O)_x$ and Na^+-(glycine)$(H_2O)_x$ as a function of *x*. Data are listed in Table S2, Supporting Information.

interactions relate to the multiply ligated geometries encountered in complex biological systems.

Metal Ion Binding Modes to the Peptides. Our studies indicate that the carbonyl is the primary binding site for alkali cations and amino acids. For Li^+ and Na^+, chelation to the amino group provides the strongest interactions with the backbone, and these can then be augmented by additional chelation with side chains, for example, methionine, phenylalanine, tyrosine, and tryptophan. In proline, the enhanced basicity of the secondary nitrogen stabilizes the zwitterionic form. For K^+, similar structures are found except for glycine and tryptophan, where chelation to the amino group does not occur. Despite differences in binding modes, we find that metal—amino acid BDEs track closely with the ligand polarizability, Figure 6. In considering interactions of metal ions with peptides or proteins, these data indicate that binding to the peptide bond will occur end-on to the carbonyl because interactions with the π-electron density of the amide linkage should be much weaker, as demonstrated above. If the peptide is sufficiently flexible and its backbone is accessible, metal ions will bind to multiple carbonyls. Interactions with side chains may augment these primary metal ion—peptide bonds. In cases where the secondary structure of the peptide ties up the carbonyl groups via hydrogen-bonding interactions (e.g., α-helices or β-sheets), metal ions will either disrupt the secondary structures or will bind predominantly to amino acid side chains.

VII. Hydration

Bare Metal Ions. The variation in metal—ligand BDEs with the number of ligands elucidates solvation phenomena. As for many other ligands, multiple ligation of the alkali ions by water leads to BDEs that gradually decline with additional waters, as shown for Li^+ and Na^+ water complexes in Figure 7. This trend can be understood by ligand—ligand steric interactions and a gradually decreasing charge on the metal ion as electron-donating ligands are added. Geometries of these complexes are determined primarily by minimizing ligand—ligand repulsion[56] such that two ligands are on opposite sides of the metal ion, three ligands are trigonal planar, and four ligands are tetrahedral. After the initial solvation shell is completed (with a size dependent on the metal ion), additional ligands can bind to outer shells, especially for a ligand such as water that can form strong hydrogen bonds.

For Mg^+ complexes,[57] the sp-hybridized electron (see discussion above) occupies a ligand site, such that (e)MgL^+ complexes have a linear geometry, (e)MgL_2^+ complexes are bent, and (e)MgL_3^+ complexes are pyramidal. Because the valence electron forces the ligands closer together than those in the alkali cation systems, the BDEs for ligands attached to Mg^+ decrease more rapidly than those for Na^+, Figure 7.

Solvation of transition-metal cations shows a very distinct progression compared to the alkali and alkaline earth metal ions. For many transition-metal ions, the second BDE is stronger or comparable to the first, for example, Cu^+ in Figure 7. As noted above, sd-hybridization places electron density originally in the valence dσ orbital into an sd-hybrid orbital localized perpendicular to the metal bonding axis. Because of the symmetry of this orbital, two ligands on opposite sides of the metal ion see the same enhanced electrostatic potential and minimal ligand—ligand interactions. The third and fourth ligand bonds to transition-metal ions are typically much weaker than those of the first and second ligands, Figure 7, such that the BDEs are comparable to those of the alkali and alkaline earth metal ions. This precipitous drop in BDEs arises because these ligands are forced to interact with the sd-electron density. Indeed, this can favor putting the third and fourth ligands in the second solvation shell for strongly hydrogen-bonding ligands.[2] In contrast to this typical pattern, which is followed by most transition-metal ions, the sequential bond energies of Mn^+ show differing patterns dependent on the ligand, evidence for a change in the electronic structure upon ligation.[1,31,35]

Metalated Amino Acids. Isolated amino acids occur in their neutral form, whereas they are zwitterionic in aqueous solution. Similar to hydration, counterions can stabilize the zwitterionic form, such as in the case of

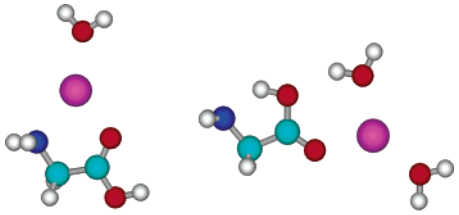

FIGURE 8. B3LYP/6-31G** optimized geometries of $(H_2O)_xNa^+$-(glycine) for $x = 1$ and 2.

M^+(proline). In contrast, M^+(glycine) retains the neutral form indicating that the strength of electrostatic interactions required to induce zwitterion formation depends on the amino acid side chain. Thus determination of the level of hydration necessary to induce solution behavior is of fundamental interest and helps determine how solvation alters the intrinsic properties of biomolecules. Recent work has begun to elucidate the thermochemistry of hydration of metalated amino acids with results available for Li^+(valine),[22,23] and Na^+(glycine).[58] Results for Na^+(glycine) are shown in Figure 7 and exhibit the same monotonic decrease as the bare alkali ions. Indeed, the first two BDEs for Na^+(glycine) essentially equal the third and fourth BDEs to Na^+, consistent with glycine remaining bidentate after hydration. Theory provides a more complete description of the geometry changes induced by hydration of Na^+(glycine), Figure 8. The first water attaches directly to Na^+, without significantly altering its interaction with glycine. In contrast, a second water molecule induces a change in the preferred binding geometry such that Na^+ attaches to the carbonyl oxygen with a water bridge to the hydroxy oxygen, Figure 8. This allows Na^+ to bind in a more optimal geometry to the carbonyl while still delocalizing electron density to the hydroxy group. (Of course, multiple conformers in such systems abound. For instance, binding of the second water molecule to Na^+ without altering the original interaction with glycine is only 4 kJ/mol higher in energy than the conformer shown in Figure 8. Other low-lying conformers have also been identified.[58]) Similar results have been obtained for hydration of the Li^+(valine) and Na^+(valine) complexes in that the binding site switches upon addition of three and two waters, respectively.[22,23] However, even four water molecules is insufficient to make the zwitterionic form of Na^+(glycine) or Na^+(valine) energetically preferred. Indeed, theory finds that addition of the first several water molecules actually destabilizes the zwitterion compared to the charge-solvated structure.[58] This is because solvation of the metal ion reduces its effective charge, thus reducing its ability to stabilize charge separation in the zwitterion. In the Na^+(glycine) system, the zwitterion cannot become the most stable geometry until both the Na^+ and NH_3^+ charge centers become solvated. In contrast, the more strongly bound and higher charge density Li^+ requires only three waters to induce a switch to a zwitterionic ground state for valine.[22,23]

VIII. Future Directions and Possibilities

Considerable progress has been made in beginning to assemble the thermodynamic "vocabulary" of metal ions interacting with small pieces of biological molecules. Extensions to other types of ligands (e.g., carbohydrates and the sugars and phosphate groups of nucleic acids) are either underway or can be anticipated soon. The assembly of this vocabulary into sentences (e.g., interactions with proteins, nucleotides, base pairs) is another imminent step in the process of making the vocabulary useful to researchers in the biological arena. Over the past 5 years, GIBMS measurements of thermochemistry using the TCID method have proven to be powerful because of the wide range of metals and ligands that can be studied and the range of BDEs accessible. The advances to date suggest that these larger molecules can be effectively studied using these and related techniques.[1,7,10,13,14]

An exciting development in this area involves multiply charged metal ions, which are of great importance in many biological systems. Experimental studies of the BDEs of ligands to multiply charged metals are still relatively few and have been restricted to values for the second solvent shell,[21,59] because the first several ligands are bound too tightly to measure by most experimental methods. An electrospray ionization (ESI) source developed for use with the GIBMS is allowing us to overcome this limitation, and BDEs for water in the first and second solvent shells of Mg^{2+} and Ca^{2+} are presently being measured. Interactions of such ions with biologically relevant molecules should follow directly.

We would like to thank the many students that contributed to this work for their dedication, insight, and hard work. Our work on metal ion interactions with biological molecules has been funded by the National Science Foundation, Grants CHE-0138504 (M.T.R.) and CHE-0135517 (P.B.A.).

Supporting Information Available: Tables of 0 K bond dissociation energies for selected metal ions with several ligands and for sequential bond energies of $(H_2O)_{x-1}M^+-H_2O$. This material is available free of charge via the Internet at http://pubs.acs.org.

References

(1) Rodgers, M. T.; Armentrout, P. B. Noncovalent metal−ligand bond energies as studied by threshold collision-induced dissociation. *Mass Spectrom. Rev.* **2000**, *19*, 215−247.
(2) Rannulu, N. S.; Rodgers, M. T. Solvation of copper ions by imidazole: Structures and sequential bond dissociation energies of Cu^+(imidazole)$_x$, $x = 1-4$, from collision-induced dissociation and theoretical studies. *Phys. Chem. Chem. Phys.*, submitted for publication.
(3) Armentrout, P. B.; Simons, J. Understanding Heterolytic Bond Cleavage. *J. Am. Chem. Soc.* **1992**, *114*, 8627−8633.
(4) Ervin, K. M.; Armentrout, P. B. Translational energy dependence of $Ar^+ + XY \rightarrow ArX^+ + Y$ (XY = H_2, D_2, HD) from thermal to 30 eV c.m. *J. Chem. Phys.* **1985**, *83*, 166−189.
(5) Schultz, R. H.; Crellin, K.; Armentrout, P. B. The sequential bond energies of $Fe(CO)_x^+$ ($x = 1-5$): Systematic effects on collision-induced dissociation measurements. *J. Am. Chem. Soc.* **1991**, *113*, 8590−8601.
(6) Rodgers, M. T.; Ervin, K. M.; Armentrout, P. B. Statistical modeling of collision-induced dissociation thresholds. *J. Chem. Phys.* **1997**, *106*, 4499−4508.
(7) Armentrout, P. B. Mass spectrometry − Not just a structural tool: The use of guided ion beam tandem mass spectrometry to determine thermochemistry. *J. Am. Soc. Mass Spectrom.* **2002**, *13*, 419−434.

(8) Rodgers, M. T. Substituent Effects in the Binding of Alkali Metal Ions to Pyridines, Studied by Threshold Collision-Induced Dissociation and ab Initio Theory: The Methylpyridines. *J. Phys. Chem. A* **2001**, *105*, 2374−2383.

(9) Gerlich, D. Inhomogeneous rf fields: A versatile tool for the study of processes with slow ions. In *State-selected and state-to-state ion−molecule reaction dynamics. Part 1: Experiment*; Ng, C.-Y., Baer, M., Eds.; Wiley: New York, 1992; pp 1−176.

(10) Armentrout, P. B. Kinetic energy dependence of ion−molecule reactions: guided ion beams and threshold measurements, *Int. J. Mass Spectrom.* **2000**, *200*, 219−241.

(11) Holbrook, K. A.; Pilling, M. J.; Robertson, S. H. *Unimolecular Reactions*; John Wiley & Sons: New York, 1996.

(12) DeTuri, V. F.; Ervin, K. M. Competitive collision-induced dissociation: gas-phase acidities and bond dissociation energies for a series of alcohols. *J. Phys. Chem. A* **1999**, *103*, 6911−6920.

(13) Koizuma, H.; Muntean, F.; Armentrout, P. B. Reactions of Cu^+ with dimethoxyethane: competition between association and multiple dissociation channels. *J. Chem. Phys.* **2004**, *120*, 756−766.

(14) Rodgers, M. T.; Armentrout, P. B. Statistical modeling of competitive threshold collision-induced dissociation. *J. Chem. Phys.* **1998**, *109*, 1787−1800.

(15) Moision, R. M.; Armentrout, P. B. Experimental and theoretical dissection of lithium cation/glycine interactions. Manuscript in preparation.

(16) Moision, R. M.; Armentrout, P. B. Experimental and theoretical dissection of sodium cation/glycine interactions. *J. Phys. Chem. A.* **2002**, *106*, 10350−10362.

(17) Moision, R. M.; Armentrout, P. B. The special five-membered ring of proline: an experimental and theoretical investigation of alkali metal cation interactions with proline and its four- and six-membered ring analogues *J. Am. Chem. Soc.*, submitted for publication.

(18) Džidić, I.; Kebarle, P. Hydration of the alkali ions in the gas phase. Enthalpies and entropies of reactions $M^+(H_2O)_{n-1} + H_2O = M^+(H_2O)_n$. *J. Phys. Chem.* **1970**, *74*, 1466−1474.

(19) Weis, P.; Kemper, P. R.; Bowers, M. T. $Mn^+(H_2)_n$ and $Zn^+(H_2)_n$ Clusters: influence of 3d and 4s orbitals on metal−ligand bonding. *J. Phys. Chem. A* **1997**, *101*, 2809−2816.

(20) Hoyau, S.; Norrman, K.; McMahon, T. B.; Ohanessian, G. A quantitative basis for a scale of Na^+ affinities of organic and small biological molecules in the gas phase. *J. Am. Chem. Soc.* **1999**, *121*, 8864−8875.

(21) Rodriguez-Cruz, S. E.; Jockusch, R. A.; Williams, E. R. Hydration energies and structures of alkaline earth metal ions, $M^{2+}(H_2O)_n$, $n = 5-7$, M = Mg, Ca, Sr, and Ba. *J. Am. Chem. Soc.* **1999**, *121*, 8898−8906.

(22) Jockusch, R. A.; Lemoff, A. S.; Williams, E. R. Effect of metal ion and water coordination on the structure of a gas-phase amino acid. *J. Am. Chem. Soc.* **2001**, *123*, 12255−12265.

(23) Jockusch, R. A.; Lemoff, A. S.; Williams, E. R. Hydration of valine-cation complexes in the gas phase: On the number of water molecules necessary to form a zwitterion. *J. Am. Chem. Soc.* **2001**, *105*, 10929−10942.

(24) Ryzhov, V.; Dunbar, R. C. Interactions of phenol and indole with metal ions in the gas phase: Models for Tyr and Trp side-chain binding. *J. Am. Chem. Soc.* **1999**, *121*, 2259−2268.

(25) Taft, R. W.; Anvia, F.; Gal, J. F.; Walsh, S.; Capon, M.; Holmes, M. C.; Hosn, K.; Oloumi, G.; Vasanwala, R.; Yazdani, S. Free energies of cation−molecule complex formation and of cation−solvent transfers. *Pure Appl. Chem.* **1990**, *62*, 17−23.

(26) Ryzhov, V.; Dunbar, R. C.; Cerda, B.; Wesdemiotis, C. Cation-π effects in the complexation of Na^+ and K^+ with Phe, Tyr, and Trp in the gas phase. *J. Am. Soc. Mass Spectrom.* **2000**, *11*, 1037−1046.

(27) Kish, M. M.; Ohanessian, G.; Wesdemiotis, C. The Na^+ affinities of α-amino acids: side-chain substituent effects *Int. J. Mass Spectrom.* **2003**, *227*, 509−524.

(28) Wilson, R. G.; Brewer, G. R. *Ion Beams*; Wiley: New York, 1973.

(29) Dalleska, N. F.; Tjelta, B. L.; Armentrout, P. B. Sequential bond energies of water to $Na^+(3s^0)$, $Mg^+(3s^1)$, and $Al^+(3s^2)$. *J. Phys. Chem.* **1994**, *98*, 4191−4195.

(30) Bauschlicher, C. W.; Sodupe, M.; Partridge, H. A theoretical study of the positive and dipositive ions of $M(NH_3)_n$ and $M(H_2O)_n$ for M = Mg, Ca, or Sr. *J. Chem. Phys.* **1992**, *96*, 4453−4463.

(31) Langhoff, S. R.; Bauschlicher, C. W.; Partridge, H.; Sodupe, M. Theoretical study of one and two ammonia molecules bound to the first-row transition metal ions. *J. Phys. Chem.* **1991**, *95*, 10677−10681.

(32) Dalleska, N. F.; Honma, K.; Sunderlin, L. S.; Armentrout, P. B. Solvation of transition metal ions by water. Sequential binding energies of $M^+(H_2O)_x$ ($x = 1-4$) for M = Ti−Cu determined by collision-induced dissociation. *J. Am. Chem. Soc.* **1994**, *116*, 3519−3528.

(33) Armentrout, P. B. Building organometallic complexes from the bare metal: Thermochemistry and electronic structure along the way. *Acc. Chem. Res.* **1995**, *28*, 430−436.

(34) Rosi, M.; Bauschlicher, C. W. The binding energies of one and two water molecules to the first transition row metal positive ions. *J. Chem. Phys.* **1989**, *90*, 7264−7272; **1990**, *92*, 1876−1878.

(35) Walter, D.; Armentrout, P. B. Sequential bond dissociation energies of $M^+(NH_3)_x$ ($x = 1-4$) for M = Ti−Cu. *J. Am. Chem. Soc.* **1998**, *120*, 3176−3187.

(36) Amunugama, R.; Rodgers, M. T. Absolute alkali metal ion binding affinities of several azines determined by threshold collision-induced dissociation and ab initio theory. *Int. J. Mass Spectrom.* **2000**, *195/196*, 439−457.

(37) Rodgers, M. T.; Armentrout, P. B. Absolute alkali metal ion binding affinities of several azoles determined by threshold collision-induced dissociation. *Int. J. Mass Spectrom.* **1999**, *185−187*, 359−380.

(38) Meyer, F.; Khan, F. A.; Armentrout, P. B. Thermochemistry of transition metal benzene complexes: Binding energies of $M(C_6H_6)_x^+$ ($x = 1, 2$) for M = Ti to Cu. *J. Am. Chem. Soc.* **1995**, *117*, 9740−9748.

(39) Bauschlicher, C. W.; Partridge, H.; Langhoff, S. R. Theoretical study of transition metal ions bound to benzene. *J. Phys. Chem.* **1992**, *96*, 3273−3278.

(40) Huang, H.; Rodgers, M. T. Sigma versus pi interactions in alkali metal ion binding to azoles. Threshold collision-induced dissociation and ab initio theory studies. *J. Phys. Chem. A* **2002**, *106*, 4277−4289.

(41) Rannula, N. S.; Rodgers, M. T. Influence of s and d orbital occupation on the binding of metal ions to imidazole. *J. Phys. Chem. A* **2004**, *108*, 6385−6396.

(42) Cerda, B. A.; Wesdemiotis, C. Li^+, Na^+ and K^+ binding to the DNA and RNA nucleobases. Bond energies and attachment sites from the dissociation of metal ion-bound heterodimers. *J. Am. Chem. Soc.* **1996**, *118*, 11884−11892.

(43) Rodgers, M. T.; Armentrout, P. B. Noncovalent interactions of nucleic acid bases (uracil, thymine, and adenine) with alkali metal ions. Threshold collision-induced dissociation and theoretical studies, *J. Am. Chem. Soc.* **2000**, *122*, 8548−8558.

(44) Yang, Z.; Rodgers, M. T. Influence of methylation on the properties of uracil and its noncovalent interactions with alkali metal ions. Threshold collision-induced dissociation and theoretical studies. *J. Am. Chem. Soc.*, submitted for publication.

(45) Yang, Z.; Rodgers, M. T. Influence of halogenation on the properties of uracil and its noncovalent interactions with alkali metal ions. Threshold collision-induced dissociation and theoretical studies. *J. Am. Chem. Soc.*, submitted for publication.

(46) Yang, Z.; Rodgers, M. T. Influence of thio-substitution on the properties of uracil and its noncovalent interactions with alkali metal ions. Threshold collision-induced dissociation and theoretical studies. Manuscript in preparation.

(47) Rodgers, M. T.; Armentrout, P. B. Influence of d orbital occupation on the binding of metal ions to adenine. *J. Am. Chem. Soc.* **2002**, *124*, 2678−2691.

(48) The interaction energy of the hydrogen bonding in an A:T pair as measured for isolated bases methylated at the glycosidic bond is about 54 kJ/mol (Yanson, I. K.; Teplitsky, A. B.; Sukhodub, L. F. Experimental studies of molecular interactions between nitrogen bases of nucleic acids. *Biopolymers* **1979**, *18*, 1149−1170).

(49) Moision, R. M.; Armentrout, P. B. Experimental and theoretical dissection of potassium cation/glycine interactions. *Phys. Chem. Chem. Phys.* **2004**, *6*, 2588−2599.

(50) Gabriel, A.; Moision, R. M.; Armentrout, P. B. Unpublished work.

(51) Ruan, C.; Rodgers, M. T. Cation-π interactions: Structures and energetics of complexation of Na^+ and K^+ with the aromatic amino acids: Phenylalanine, tyrosine and tryptophan. *J. Am. Chem. Soc.*, in press.

(52) Cerda, B. A.; Wesdemiotis, C. The relative copper (I) ion affinities of amino acids in the gas phase. *J. Am. Chem. Soc.* **1995**, *117*, 9734−9739.

(53) Gapeev, A.; Dunbar, R. C. Na^+ affinities of gas-phase amino acids by ligand exchange equilibrium. *Int. J. Mass Spectrom.* **2003**, *228*, 825−839.

(54) Klassen, J. S.; Anderson, S. G.; Blades, A. T.; Kebarle, P. Reaction enthalpies for $M^+L = M^+ + L$, where $M^+ = Na^+$ and K^+ and L = acetamide, *N*-methylacetamide, N, N-dimethylacetamide, glycine, and glycylglycine, from determinations of the collision-induced dissociation thresholds. *J. Phys. Chem.* **1996**, *100*, 14218−14227.

(55) Cerda, B. A.; Hoyau, S.; Ohanessian, G.; Wesdemiotis, C. Na^+ binding to cyclic and linear dipeptides. Bond energies, entropiesof Na^+ complexation, and attachment sites from the dissociation of Na^+-bound heterodimers and ab initio calculations. *J. Am. Chem. Soc.* **1998**, *120*, 2437−2448.
(56) Bauschlicher, C. W.; Langhoff, S. R.; Partridge, H.; Rice, J. E.; Komornicki, A. A theoretical study of $Na(H_2O)_n^+$ (n = 1−4). *J. Chem. Phys.* **1991**, *95*, 5142−5148.
(57) Andersen, A.; Muntean, F.; Walter, D.; Rue, C.; Armentrout, P. B. Collision-induced dissociation and theoretical studies of Mg^+ complexes with CO, CO_2, NH_3, CH_4, CH_3OH, and C_6H_6. *J. Phys. Chem. A* **2000**, *104*, 692−705.
(58) Ye, S.; Moision, R. M.; Armentrout, P. B. Sequential bond energies of water to sodium glycine cation. *Int. J. Mass Spectrom.*, in press.
(59) Peschke, M.; Blades, A. T.; Kebarle, P. Hydration energies and entropies for Mg^{2+}, Ca^{2+}, Sr^{2+}, and Ba^{2+} from gas-phase ion−water molecule equilibria determinations. *J. Phys. Chem. A* **1998**, *102*, 9978−9985.

AR0302843